Controls on the tropospheric oxidizing capacity during an idealized Dansgaard-Oeschger event, and their implications for the rapid rises in atmospheric methane during the last glacial period

J. G. Levine,[1] E. W. Wolff,[1] P. O. Hopcroft,[2] and P. J. Valdes[2]

Received 30 March 2012; revised 30 May 2012; accepted 6 June 2012; published 28 June 2012.

[1] The ice core record reveals large variations in the concentration of atmospheric methane, [CH_4], over the last 800 kyr. Amongst the most striking natural features are the large, rapid rises in [CH_4], of 100–200 ppbv, on timescales of less than 100 years, at the beginning of Dansgaard-Oeschger (D-O) events during the last glacial period (21–110 kyr before present). Despite the potential insight they could offer into the likelihood of future rapid rises in [CH_4], the relative roles of changes in methane sources and sinks during D-O events have been little explored. Here, we use a global atmospheric chemistry-transport model to explore—for the first time, in a process-based fashion—controls on the oxidizing capacity during an idealized D-O event that features a characteristically rapid rise in [CH_4]. We find that the two controls previously identified in the literature as having had significant (though opposing) influences on the oxidizing capacity between glacial and interglacial periods—changes in air temperature and emissions of non-methane volatile organic compounds from vegetation—offset one another between idealized Heinrich stadial and Greenland interstadial states. The result is, the net change in oxidizing capacity is very small, implying the rapid rises in [CH_4] at the beginning of D-O events were almost entirely source-driven. This poses a challenge to earth-system models—to generate a sufficiently large increase in methane emissions in response to a simulated D-O event, via a more realistic freshwater forcing impacting the strength of the Atlantic meridional overturning circulation or, possibly, other climate-change mechanisms. **Citation:** Levine, J. G., E. W. Wolff, P. O. Hopcroft, and P. J. Valdes (2012), Controls on the tropospheric oxidizing capacity during an idealized Dansgaard-Oeschger event, and their implications for the rapid rises in atmospheric methane during the last glacial period, *Geophys. Res. Lett.*, *39*, L12805, doi:10.1029/2012GL051866.

1. Introduction

[2] Methane (CH_4) is a potent greenhouse gas and influences the tropospheric oxidizing capacity. Straddling issues of composition and climate, attempts to explain past changes in its budget test our understanding of the earth system. We know from the ice record that its concentration, [CH_4], has varied greatly over the last 800 kyr [e.g., *Loulergue et al.*, 2008], some of the most striking natural features being: the differences in [CH_4] between glacial and interglacial periods, for example rising from about 360 ppbv at the Last Glacial Maximum (LGM; ∼21 kyr before present (BP)) to around 700 ppbv in the pre-industrial era (PI; ∼200 yr BP); and the 100–200 ppbv excursions from the last glacial 'baseline' of 355–460 ppbv, towards interglacial values, at the beginning of Dansgaard-Oeschger (D-O) events (between 21 and 110 kyr BP). Whilst there has been much debate regarding the relative roles of changes in CH_4 sources and sinks between the LGM and the PI [e.g., *Chappellaz et al.*, 1993; *Valdes et al.*, 2005; *Kaplan et al.*, 2006; *Fischer et al.*, 2008; *Singarayer et al.*, 2011; *Levine et al.*, 2011a, 2011b], the D-O excursions in [CH_4] have received less attention [*Flückiger et al.*, 2004; *Huber et al.*, 2006; *Bock et al.*, 2010; *Hopcroft et al.*, 2011]. The latter, however, are of particular interest regarding possible future changes in [CH_4], as they exhibit initial, rapid rises in [CH_4], on timescales of less than 100 years. Here, we carry out a series of experiments with an atmospheric chemistry-transport model to explore controls on the oxidizing capacity during an idealized D-O event featuring a characteristically rapid rise in [CH_4] [*Hopcroft et al.*, 2011].

[3] *Hopcroft et al.* [2011] simulated the idealized D-O event with the Fast Met Office UK Universities Simulator (FAMOUS) [*Jones et al.*, 2005; *Smith et al.*, 2008], forced with a prescribed cycle in freshwater flux (+/−0.5 Sv). They used climate data from FAMOUS to force the Sheffield Dynamic Global Vegetation Model (SDGVM) [*Woodward et al.*, 1995; *Beerling and Woodward*, 2001], and output from this to drive a model of wetlands [*Cao et al.*, 1996] and a model of volatile organic compound (VOC) emissions [*Guenther et al.*, 1995]. They thereby simulated the evolution of CH_4 and non-methane VOC (NMVOC) emissions. Though their base simulation showed many of the essential features of observed D-O events, such as substantial changes in Greenland temperature, it proved difficult to capture their full scale. Regarding CH_4, their base simulation captured the rapidity of the initial rise in [CH_4] but, based on changes in CH_4 emissions alone, an increase in [CH_4] from an idealized Heinrich stadial (HS) state to an idealized Greenland interstadial (GI) state—an upper estimate of the increase in [CH_4] at the beginning of a D-O event—of just 56 ppbv. Though they estimated that this would increase to one of 61–66 ppbv as a result of the influence of changes in NMVOC emissions from vegetation on the lifetime of methane, τ_{CH_4} (using a semi-empirical relationship between τ_{CH_4} and the amount of isoprene emitted annually), it remained short of the 100–200 ppbv excursions typically

[1]British Antarctic Survey, Cambridge, UK.
[2]Bristol Research Initiative for the Dynamic Global Environment, University of Bristol, Bristol, UK.

Corresponding author: J. G. Levine, British Antarctic Survey, High Cross, Madingley Road, Cambridge CB3 0ET, UK. (javi@bas.ac.uk)

0094-8276/12/2012GL051866

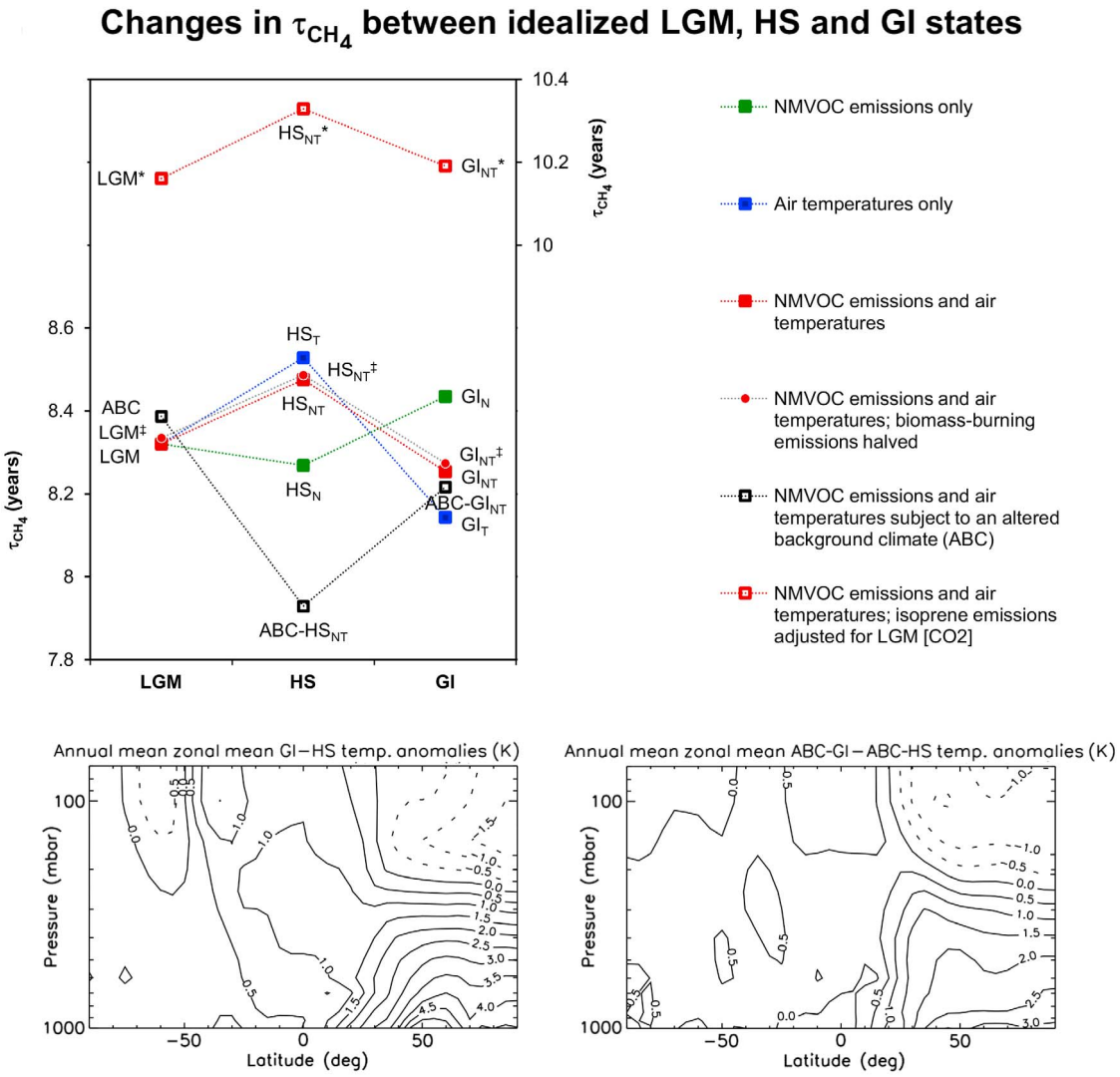

Figure 1. (top) Modeled changes in methane lifetime (τ_{CH_4}) between idealized Last Glacial Maximum (LGM), Heinrich stadial (HS) and Greenland interstadial (GI) states [*Hopcroft et al.*, 2011], in response to changes in non-methane volatile organic compound (NMVOC) emissions from vegetation and/or changes in air temperatures; ABC refers to an altered background climate employing LGM [CO_2] but 84 kyr BP orbital insolation and pre-industrial land ice. (bottom left) GI – HS and (bottom right) ABC-GI – ABC-HS annual mean zonal mean temperature anomalies.

observed [e.g., *Spahni et al.*, 2005]. Only by unrealistically altering their background climate, employing LGM [CO_2] (185 ppmv) but 84 kyr BP orbital insolation and PI land ice, could they simulate a source-driven increase in [CH_4] of around 110 ppbv, and an increase of 160 ppbv on including the influence of NMVOC emissions. *Hopcroft et al.* [2011] suggested the shortfall could have been the result of: an underestimation of the climate-sensitivity of CH_4 sources; incomplete/incorrect freshwater forcing; and/or erroneous assumptions regarding τ_{CH_4}. Here, we explore what was an implicit assumption regarding τ_{CH_4}, that the only significant effect the climate has on τ_{CH_4} (besides that induced by changes in CH_4 emissions, which we consider to be part of source-driven changes in [CH_4]) is that which it exerts via changes in NMVOC emissions from vegetation (from here on, referred to simply as NMVOC emissions).

[4] Calculations by *Levine et al.* [2011a] suggested the influence on τ_{CH_4} of changes in NMVOC emissions between the LGM and the PI was all but negated by two physical effects of the changes in air temperature accompanying these: the lower air temperatures of the LGM were responsible for reduced [OH], due to reduced humidities, and altered chemical kinetics, including a reduction in the reactivity that OH shows towards CH_4, that together compensated for the increase in [OH] due to reduced NMVOC emissions at the LGM [see, e.g., *Valdes et al.*, 2005; *Kaplan et al.*, 2006]. Furthermore, previous calculations by *Harder et al.* [2007] illustrated the sensitivity that τ_{CH_4} shows to

the degree of glacial cooling. Whilst *Hopcroft et al.* [2011] included the influence of changes in NMVOC emissions in their calculations, extending their base GI-HS increase in [CH_4] from 56 ppbv to 61–66 ppbv (depending on whether or not they adjusted their isoprene emissions for reduced CO_2-inhibition at the LGM according to *Possell et al.* [2005]), they did not explore the physical effects of the changes in air temperature between HS and GI states. The inclusion of these effects could yield an even lower estimate of the increase in [CH_4] at the beginning of a D-O event, focusing further attention on the climate-sensitivity of CH_4 sources captured by models, and the freshwater forcing of D-O events. The implication of *Levine et al.*'s [2011a] findings was that the change in [CH_4] between the LGM and the PI was almost entirely source-driven—a conclusion consistent with the most recent estimates of the changes in CH_4 sources during that period [e.g., *Weber et al.*, 2010]. We are therefore interested to explore to what extent these controls on the oxidizing capacity continue to compensate for each other between idealized LGM, HS and GI states—subject to different drivers, and consequently different patterns, of climate change.

[5] In contrast to the concomitant changes in air temperatures, greenhouse-gas concentrations and surface albedo that drove the last deglaciation [see, e.g., *Singarayer and Valdes*, 2010; *Köhler et al.*, 2010], the D-O climate changes are believed to have been the result of changes in ocean circulation, and hence global heat distribution, driven by changes in freshwater flux [e.g., *Ganopolski and Rahmstorf*, 2001; *Clark et al.*, 2002; *McManus et al.*, 2004]. Instead of air temperatures (as reflected in $\delta^{18}O$) changing in a roughly symmetrical manner about the equator, with LGM-to-PI warmings of the same order of magnitude in Greenland and Antarctica, the changes in air temperature accompanying D-O events were much larger in Greenland than the Antarctic and, at any one time, largely of opposite sign (hence the so-called 'bipolar see-saw') [e.g., *Blunier and Brook*, 2001]. The D-O temperature changes simulated by *Hopcroft et al.* [2011] are largely confined to the northern hemisphere and, from the HS to the GI, comprise an average warming in the tropics (the most influential region for CH_4 oxidation [see, e.g., *Lawrence et al.*, 2001]) of about 1 K in their base simulation (and 0.4 K subject to their altered background climate); see Figure 1. A different atmosphere–ocean general circulation model (AOGCM) would likely yield somewhat different temperature changes but, in response to a 1 Sv freshwater forcing, albeit with a smaller temperature change over Greenland, FAMOUS shows broadly similar temperature changes to HadCM3 (the Hadley Centre Model on which it is based) and HadCM3's response compares well with the AOGCM ensemble mean presented by *Stouffer et al.* [2006] [see *Hopcroft et al.*, 2011]. Compared to the 2.5 K tropical warming that *Levine et al.* [2011a] explored between the LGM and the PI [see *Levine et al.*, 2011a, Figure 1b], 1 K and 0.4 K warmings are small, and we therefore expect the temperature effects between HS and GI states to be small. But the question is, to what extent these effects compensate for the accompanying changes in NMVOC emissions, the latter also being smaller than previously explored by *Levine et al.* [2011a]: *Hopcroft et al.*'s [2011] base simulation yielded a 10% increase in isoprene emissions from the HS to the GI (and their simulation subject to an altered background climate yielded an increase of 30%), compared to *Valdes et al.*'s [2005] 160% increase from the LGM to the PI (partly in response to a large increase in CO_2-fertilization).

2. Model Experiments

[6] To explore the competing controls on the oxidizing capacity, we carry out a series of experiments with the Cambridge parallelised-Tropospheric Offline Model of Chemistry and Transport (p-TOMCAT). This is a 3D global Eulerian model, run here at a resolution of $5.6° \times 5.6°$ on 31 levels, stretching from the surface to 10 hPa. In a similar manner to *Levine et al.* [2011a], we drive the model with a combination of meteorological data from operational analyses of the European Centre for Medium-range Weather Forecasts (ECMWF) and *Hopcroft et al.*'s [2011] LGM, HS and GI simulations: adopting *Hopcroft et al.*'s [2011] air temperatures, we recalculate the saturated water vapor volume mixing ratios with respect to ice according to *Marti and Mauersberger* [1993], and adjust the water vapor volume mixing ratios from their ECMWF counterparts to conserve relative humidity. The model's chemistry includes the HO_x/NO_x chemistries of methane, ethane, propane and isoprene, with the oxidation of isoprene following the Mainz Isoprene Mechanism [*Pöschl et al.*, 2000]. There has been much discussion regarding the possible recycling of OH consumed in isoprene oxidation [e.g., *Lelieveld et al.*, 2008], with a mechanism based on the theoretical calculations of *Peeters et al.* [2009] showing significant potential to reconcile discrepancies between modeled and measured [OH] in regions of high isoprene (and low NO_x) emissions [e.g., *Archibald et al.*, 2011]. Previous experiments with p-TOMCAT, however, suggest this mechanism would have had little impact on τ_{CH_4} at the LGM and changes in τ_{CH_4} due to changes in NMVOC emissions and air temperatures [*Levine et al.*, 2011a], and we therefore do not explore it further here.

[7] With three exceptions, the basic model setup is identical to that used by *Levine et al.* [2011a, 2011b]: two of the 'lumped' species in the Mainz Isoprene Mechanism [*Pöschl et al.*, 2000], ISO_2 and $MACRO_2$, are advected as tracers as opposed to being treated as steady-state species; a diurnal cycle is imposed on the emissions of isoprene; and we adopt the updated chemical rate coefficients and parameters governing wet- and dry deposition rates used in the UKCA global chemistry-climate model by *Archibald et al.* [2011]. (For reference, these changes were found to increase τ_{CH_4} by 5%.) Additionally, instead of emitting CH_4, we fix [CH_4] = 355 ppbv throughout the model, in all experiments—the volume mixing ratio that *Hopcroft et al.* [2011] employed in their LGM climate simulation. This permits a relatively short 'spin-up' of two years in each experiment, before running for a third year to calculate τ_{CH_4}, defined as the average value of k_{OH}.[OH] (where k_{OH} is the rate coefficient for the reaction between OH and CH_4) throughout the troposphere (defined by the 380 K/2 PVU tropopause), weighted according to the mass of CH_4 exposed to that value of k_{OH}.[OH]. τ_{CH_4} is thus the e-folding lifetime of tropospheric CH_4 with respect to OH.

[8] Summarized in Table 1, the main experiments comprise an LGM integration, employing *Hopcroft et al.*'s [2011] LGM NMVOC emissions and air temperatures, and three pairs of HS and GI integrations in which we change, only the NMVOC emissions (HS_N and GI_N), only the air

Table 1. Main Features of Model Experiments, and the CH_4 Lifetimes Calculated Therein (τ_{CH_4}); $\Delta\tau_{CH_4}$ is the Percentage Change in τ_{CH_4} in Each Experiment Relative to the Corresponding LGM Experiment[a]

Experiment	Air temp's	NMVOC emissions	τ_{CH_4} (years)	$\Delta\tau_{CH_4}$ (%)	Notes
LGM	LGM	LGM	8.3	-	-
HS_N	LGM	HS	8.3	−0.6	-
GI_N	LGM	GI	8.4	+1.4	-
HS_T	HS	LGM	8.5	+2.5	-
GI_T	GI	LGM	8.1	−2.1	-
HS_{NT}	HS	HS	8.5	+1.9	-
GI_{NT}	GI	GI	8.3	−0.8	-
LGM*	LGM	LGM*	10.2	-	*Isoprene emissions adjusted for reduced CO_2-inhibition [*Possell et al.*, 2005]
HS_{NT}*	HS	HS*	10.3	+1.7	
GI_{NT}*	GI	GI*	10.2	−0.3	
LGM‡	LGM	LGM	8.3	-	‡Biomass-burning emissions halved from PI levels [*Valdes et al.*, 2005]
$HS^{‡}_{NT}$	HS	HS	8.5	+1.8	
$GI^{‡}_{NT}$	GI	GI	8.3	−0.7	
ABC	ABC	ABC	8.2	-	Air temperatures and NMVOC emissions simulated subject to altered background climate (ABC)
ABC-HS_{NT}	ABC-HS	ABC-HS	7.9	−3.8	
ABC-GI_{NT}	ABC-GI	ABC-GI	8.1	−1.3	

[a]For example, in HS_{NT} relative to LGM, or in HS_{NT}* relative to LGM*.

temperatures (HS_T and GI_T), and both the NMVOC emissions and air temperatures (HS_{NT} and GI_{NT}), in line with their HS and GI simulations. The emissions of isoprene employed in the main experiments are not adjusted for reduced CO_2-inhibition at the LGM, however, as a sensitivity test, we repeat the LGM, HS_{NT} and GI_{NT} experiments subject to adjustment for LGM [CO_2] (185 ppmv) according to *Possell et al.* [2005] (LGM*, HS_{NT}* and GI_{NT}*); see Table 2. We also repeat the LGM, HS_{NT} and GI_{NT} experiments subject to a 50% reduction in biomass-burning emissions from their values in Table 2 (LGM‡, $HS^{‡}_{NT}$ and $GI^{‡}_{NT}$) for reasons given below. As a further (extreme) sensitivity test, we also repeat the LGM, HS_{NT} and GI_{NT} experiments subject to the air temperatures and NMVOC emissions simulated by *Hopcroft et al.* [2011] subject to their (unrealistically) altered background climate employing LGM [CO_2] but 84 kyr BP orbital insolation and PI land ice (ABC, ABC-HS_{NT} and ABC-GI_{NT}), with which they obtained their greatest source-driven increase in [CH_4] from HS to GI. All of the emission/temperature data that we employ comprise 30-year climatological monthly-means. Note that some of the data differ somewhat from those quoted by *Hopcroft et al.* [2011]—for example, our HS isoprene emissions (not adjusted for reduced CO_2-inhibition at the LGM) total 284.7 Tg C $year^{-1}$, compared to their 281.9 Tg C $year^{-1}$—as it was necessary to rerun FAMOUS (not bit-reproducible) to archive some of the data for this study.

[9] Aside from the NMVOC emissions, all other trace gas emissions are kept constant throughout the experiments; see Table 2. We employ *Valdes et al.*'s [2005] LGM oceanic, soil and lightning emissions, though the latter are coupled in time and space to our parameterization of convection [*Stockwell et al.*, 1999] and therefore distributed somewhat differently. Regarding biomass burning emissions, top-down Monte Carlo calculations by *Fischer et al.* [2008], designed to explain observed changes in [CH_4], $\delta^{13}CH_4$ and $\delta D(CH_4)$, suggest there was a similar amount of biomass burning at the LGM as in the PI, however the few charcoal records that span the LGM suggest there was less biomass burning between 16 and 21 kyr BP than in the PI [*Power et al.*, 2008]. Therefore, though we primarily employ *Valdes et al.*'s [2005] PI biomass-burning emissions, we also explore the sensitivity of our results to a 50% reduction in these (experiments LGM‡, $HS^{‡}_{NT}$ and $GI^{‡}_{NT}$); note, we do not

Table 2. Trace-Gas Emissions Based on *Valdes et al.* [2005] and *Hopcroft et al.* [2011], As Outlined in the Text[a]

			Vegetation					Total		
Trace Gas	Biomass Burning	Ocean	LGM	HS	GI	Soils	Lightning	LGM	HS	GI
NO_2	1.4	-	-	-	-	5.7	3.4	10.5	10.5	10.5
CO	100.0	41.2	100.5	94.7	105.4	-	-	241.7	235.9	246.6
CO[b]	100.0	41.2	142.7	95.7	127.7	-	-	283.9	236.9	268.9
C_2H_6	0.7	-	2.3	2.2	2.4	-	-	3.0	2.9	3.1
C_2H_6[b]	0.7	-	3.3	2.3	2.9	-	-	4.0	3.0	3.6
C_3H_8	0.2	0.4	2.3	2.2	2.4	-	-	2.9	2.8	3.0
C_3H_8[b]	0.2	0.4	3.3	2.3	2.9	-	-	3.9	2.9	3.5
CH_3COCH_3	0.1	-	13.4	12.6	14.0	-	-	13.5	12.7	14.1
CH_3COCH_3[b]	0.1	-	19.0	12.8	17.0	-	-	19.1	12.9	17.1
C_5H_8	-	-	330.0	322.7	353.6	-	-	330.0	322.7	353.6
C_5H_8[c]	-	-	770.4	753.3	825.5	-	-	770.4	753.3	825.5
C_5H_8[b]	-	-	468.7	345.8	444.7	-	-	468.7	345.8	444.7
HCHO	0.3	-	-	-	-	-	-	0.3	0.3	0.3
CH_3CHO	0.8	-	-	-	-	-	-	0.8	0.8	0.8

[a]Tg molecular mass $year^{-1}$; except for NO_2 in Tg N $year^{-1}$.
[b]Simulated subject to an altered background climate (ABC).
[c]Adjusted for CO_2-inhibition according to *Possell et al.* [2005].

explore changes in biomass-burning emissions of CH_4, as we fix $[CH_4]$ = 355 ppbv.

3. Results

[10] The τ_{CH_4} calculated in each experiment is given in Table 1 and illustrated in Figure 1. In the HS state (forced by a 0.5 Sv increase in freshwater flux, leading to a weaker Atlantic meridional overturning circulation and lower Greenland temperatures), global NMVOC emissions and tropical air temperatures are lower than at the LGM. The reduction in NMVOC emissions reduces τ_{CH_4} by 0.6% (HS_N), whilst the reduction in air temperatures increases τ_{CH_4} by 2.5% (HS_T), resulting in a net increase of 1.9% (HS_{NT}). The influence of air temperatures thus more than compensates for the influence of NMVOCs; see Figure 1.

[11] In the GI state (forced by a 0.5 Sv reduction in freshwater flux, leading to a stronger Atlantic meridional overturning circulation and higher Greenland temperatures), global NMVOC emissions and tropical air temperatures are higher than at the LGM. The increase in NMVOC emissions increases τ_{CH_4} by 1.4% (GI_N), whilst the increase in air temperatures reduces τ_{CH_4} by 2.1% (GI_T), resulting in a net reduction of 0.8% (GI_{NT}). Again, the influence of air temperatures dominates; see Figure 1. Accordingly, the net effect of the increase in NMVOC emissions and air temperatures from HS_{NT} to GI_{NT} comprises a 2.6% reduction in τ_{CH_4}. This is a very small net change, translating to just a 9 ppbv reduction in $[CH_4]$. Note, however, that this would slightly offset, as opposed to extend, the 56 ppbv source-driven increase in $[CH_4]$ calculated by *Hopcroft et al.* [2011], making it still harder to account for the 100–200 ppbv excursions observed.

[12] Adjusting the emissions of isoprene for reduced CO_2-inhibition at the LGM increases τ_{CH_4} in LGM*, HS_{NT}* and GI_{NT}* by around 22% relative to LGM, HS_{NT} and GI_{NT} respectively. However, our main findings are largely unaffected: the influence of air temperatures dominates, and we estimate that the net effect on the oxidizing capacity from the HS to the GI (from HS_{NT}* to GI_{NT}*) amounts to a 2.0% reduction in τ_{CH_4}, translating to a 7 ppbv reduction in $[CH_4]$. Halving the biomass-burning emissions has almost no effect on τ_{CH_4} in LGM‡, $HS^{\ddagger}_{NT}$ and $GI^{\ddagger}_{NT}$ relative to LGM, HS_{NT} and GI_{NT} respectively, and akin to from HS_{NT} to GI_{NT}, we obtain a net reduction in τ_{CH_4} of 2.5%, translating to a 9 ppbv reduction in $[CH_4]$, from $HS^{\ddagger}_{NT}$ to $GI^{\ddagger}_{NT}$.

[13] Employing the NMVOC emissions and air temperatures simulated by *Hopcroft et al.* [2011] subject to their altered background climate, we calculate a net increase in τ_{CH_4} from ABC-HS_{NT} to ABC-GI_{NT} of 3.6%, translating to a 12 ppbv increase in $[CH_4]$. Note that subject to this unrealistic background climate, the net effect on the oxidizing capacity switches sign but remains very small; it would extend the 110 ppbv source-driven increase in $[CH_4]$ that *Hopcroft et al.* [2011] calculated, but only slightly.

4. Summary and Discussion

[14] Our experiments with the Cambridge p-TOMCAT model suggest the net effect on τ_{CH_4} of the changes in NMVOC emissions and air temperatures between idealized HS and GI states [*Hopcroft et al.*, 2011] is very small (less than 3%), owing to their small and opposing individual influences. As outlined in section 1, we would expect a different AOGCM, subject to the same freshwater forcing, to yield somewhat different temperature changes: the precise temperature changes are uncertain. However, we would generally expect a greater (lesser) HS-to-GI warming to result in a greater (lesser) increase in NMVOC emissions, and hence the continued offsetting of one influence against the other. We therefore consider the very small net change in τ_{CH_4} a robust result. This has implications for the cause(s) of the rapid rises in $[CH_4]$ observed at the beginning of D-O events, and our current ability (or inability) to account for these via a 'bottom-up' modelling approach. It is also interesting that, in most of our calculations, the influence of air temperatures comprises the dominant control on the oxidizing capacity. We discuss these points below, comparing/contrasting our findings with those of a recent 'top-down' study by *Bock et al.* [2010] combining measurements of $[CH_4]$ and $\delta D(CH_4)$ spanning D-O events 7 and 8 (33–41 kyr BP) with a simple box model.

[15] The very small net change in oxidizing capacity between idealized HS and GI states suggests the D-O excursions in $[CH_4]$ were almost entirely source-driven. This contrasts with *Bock et al.*'s [2010] explanation of the excursions in $[CH_4]$ accompanying D-O events 7 and 8, which invoked about a 10% increase in τ_{CH_4} between stadial and early-interstadial states, in addition to roughly a 20% increase in CH_4 emissions; see Table S2 of their Supporting Online Material (SOM). We find no grounds for such an increase in τ_{CH_4} here. In principle, other factors besides those we have explored could have influenced the oxidizing capacity, such as changes in albedo, cloudiness, stratospheric ozone and NO_x emissions. As discussed by *Levine et al.* [2011a], there is as yet no evidence in the literature that these factors had much influence on τ_{CH_4} between the LGM and the PI (and in the case of NO_x emissions, even an influence of the 'right' sign), and it is by no means obvious how they might have made a more significant contribution to the D-O excursions in $[CH_4]$—these being the result of smaller changes in climate. However, our timeslice experiments may not fully capture all transient changes in the earth system, the temporal and spatial resolution of which could shed further light on the cause(s) of the D-O excursions. If entirely source-driven, the observed D-O excursions of 100–200 ppbv, from a glacial baseline of 355–460 ppbv, reflect increases in total CH_4 emissions of 20-50% (allowing for a 10% positive feedback between $[CH_4]$ and τ_{CH_4}). It follows that the 20% increase in total CH_4 emissions estimated by *Bock et al.* [2010] could account for an excursion of 100 ppbv, but not one of 200 ppbv. Even explaining this 20% increase is challenging, as it was underpinned by a 33% increase in CH_4 emissions from wetlands (see Table 2 of Bock et al.'s SOM) and *Hopcroft et al.* [2011] calculated just a 14.3% increase in wetland emissions in their base simulation and an increase of 30% only by unrealistically altering their background climate.

[16] Accounting for D-O excursions of 200 ppbv therefore poses a challenge. However, one of *Bock et al.*'s [2010] findings could inform future modelling efforts, namely that synchronous changes in $\delta D(CH_4)$ and the inter-hemispheric gradient in $[CH_4]$ could only be explained by a far larger increase in CH_4 emissions from boreal wetlands than from tropical wetlands: an increase of 400% or 24 Tg CH_4 $year^{-1}$ (from 6 to 30 Tg CH_4 $year^{-1}$) compared to one of 7% or

6 Tg CH_4 $year^{-1}$ (from 84 to 90 Tg CH_4 $year^{-1}$); see Table S2 of Bock et al.'s SOM. *Hopcroft et al.*'s [2011] base simulation yielded a not dissimilar increase in the tropics of 10% or 6.6 Tg CH_4 $year^{-1}$ (from 65.4 to 72.0 Tg CH_4 $year^{-1}$), but an increase north of 30°N—comparable with the 'boreal region' in *Bock et al.*'s [2010] simple box model—of just 34% or 9.6 Tg CH_4 $year^{-1}$ (from 28.2 to 37.8 Tg CH_4 $year^{-1}$); their simulation subject to an altered background climate yielded an increase of 18% or 10.1 Tg CH_4 $year^{-1}$ (from 56.8 to 66.9 Tg CH_4 $year^{-1}$) north of 30°N. This suggests that *Hopcroft et al.*'s [2011] models underestimated the increase in boreal wetland emissions. Further work will be needed to elucidate the cause(s) of this underestimate but it is possible that it was partly the result of an overestimation of boreal wetland emissions in the HS state (28.2 Tg CH_4 $year^{-1}$ in their base simulation c.f. 6 Tg CH_4 $year^{-1}$ estimated by *Bock et al.* [2010]); we note that the SDGVM does not include the effect of soil-water freezing on plant productivity. However, very recent high-resolution [CH_4] records from the North Greenland Ice Core Project (NGRIP) and European Project for Ice Coring in Antarctica – Dronning Maud Land (EDML) ice cores [*Baumgartner et al.*, 2012] suggest there was generally a greater inter-hemispheric gradient at and around the LGM, between about 17 and 27 kyr BP, than previously supposed [*Dällenbach et al.*, 2000]. It is therefore possible that the boreal wetlands were more active in stadial conditions than *Bock et al.* [2010] estimated, and *Hopcroft et al.*'s [2011] HS estimate may be less of an overestimate. It would be interesting to see if boreal peat records could offer some constraint on just how low boreal wetland emissions were under stadial conditions. Additionally, it is likely that their underestimate of the increase in boreal wetland emissions was partly the result of simulating too small a change in climate between idealized HS and GI states: *Hopcroft et al.* [2011] noted that their simulations yielded smaller Greenland warmings than typically observed (6–8°C c.f. 8–16°C), albeit accompanied by somewhat larger warmings in the North Atlantic. The challenge here will be to generate a sufficiently large change in climate: a realistic freshwater forcing may not be enough and other climate-change mechanisms may be required to reproduce observations.

[17] Finally, though the influence that NMVOCs such as isoprene have on τ_{CH_4} has been widely recognized by the paleoscience community following the studies of *Valdes et al.* [2005] and *Kaplan et al.* [2006], the influence of air temperatures has not, or at least not consistently. Here, we find that the latter can be not just of comparable magnitude [see, e.g., *Levine et al.*, 2011a], but the dominant control on the oxidizing capacity. *Valdes et al.* [2005] explored the influence of air temperatures (as well as NMVOCs) between the LGM and the PI, but *Kaplan et al.* [2006] did not, and notably, neither did *Singarayer et al.* [2011] in their recent study of [CH_4] spanning the last glacial-interglacial cycle (the last 130 kyr). Had *Singarayer et al.* [2011] done so, their simulated [CH_4] curve would likely have retained much of its overall shape, and perhaps the timing of [CH_4] variations contained therein, but it would not have captured as much of the amplitude of [CH_4] variation evident from the ice record; the influence of air temperatures would have at least partly offset the [CH_4] variation gained on including the influence of NMVOC emissions; see Figure S4 of Singarayer et al.'s Supplementary Information. In future studies, we suggest that if one influence is included, so must the other; after all, NMVOC emissions are part-determined by air temperatures—both in terms of net primary productivity, governing the amount of vegetation available to emit NMVOCs [e.g., *Lieth*, 1975], and the amount of NMVOCs emitted per unit leaf area [e.g., *Guenther et al.*, 1995].

[18] **Acknowledgments.** This study is part of the British Antarctic Survey Polar Science for Planet Earth Programme and a contribution to the Dynamics of the Earth System and the Ice-core Record project, the latter being jointly funded by the Natural Environment Research Council's programme, Quantifying and Understanding the Earth System, and the French Institut National des Sciences de l'Univers; we gratefully acknowledge their support. We also express our thanks to Anna Jones of the British Antarctic Survey for helpful discussions in the preparation of this manuscript, and Glenn Carver and the Centre for Atmospheric Science, University of Cambridge, for their support in using the Cambridge p-TOMCAT model. Finally, we thank Jed Kaplan and an anonymous reviewer for their constructive comments on this paper.

[19] The Editor thanks Jed Kaplan and an anonymous reviewer for assisting in the evaluation of this paper.

References

Archibald, A. T., et al. (2011), Impacts of HO_x regeneration and recycling in the oxidation of isoprene: Consequences for the composition of past, present and future atmospheres, *Geophys. Res. Lett.*, *38*, L05804, doi:10.1029/2010GL046520.

Baumgartner, M., et al. (2012), High-resolution interpolar difference of atmospheric methane around the Last Glacial Maximum, *Biogeosci. Discuss.*, *9*, 5471–5508, doi:10.5194/bgd-9-5471-2012.

Beerling, D. J., and F. I. Woodward (2001), *Vegetation and the Terrestrial Carbon Cycle, Modelling the First 400 Million Years*, Cambridge Univ. Press, New York, doi:10.1017/CBO9780511541940.

Blunier, T., and E. J. Brook (2001), Timing of millennial-scale climate change in Antarctica and Greenland during the last glacial period, *Science*, *291*, 109–112, doi:10.1126/science.291.5501.109.

Bock, M., et al. (2010), Hydrogen isotopes preclude marine hydrate CH_4 emissions at the onset of Dansgaard-Oeschger events, *Science*, *328*, 1686–1689, doi:10.1126/science.1187651.

Cao, M., S. Marshall, and K. Gregson (1996), Global carbon exchange and methane emissions from natural wetlands: application of a process-based model, *J. Geophys. Res.*, *101*(D9), 14,399–14,414, doi:10.1029/96JD00219.

Chappellaz, J. A., et al. (1993), The atmospheric CH_4 increase since the Last Glacial Maximum, (1). Source estimates, *Tellus, Ser. B*, *45*, 228–241, doi:10.1034/j.1600-0889.1993.t01-2-00002.x.

Clark, P., et al. (2002), The role of the thermohaline circulation in abrupt climate change, *Nature*, *415*, 863–869, doi:10.1038/415863a.

Dällenbach, A., T. Blunier, J. Flückiger, B. Stauffer, J. Chappellaz, and D. Raynaud (2000), Changes in the atmospheric CH_4 gradient between Greenland and Antarctica during the Last Glacial and the transition to the Holocene, *Geophys. Res. Lett.*, *27*(7), 1005–1008, doi:10.1029/1999GL010873.

Fischer, H., et al. (2008), Changing boreal methane sources and constant biomass burning during the last termination, *Nature*, *452*, 864–867, doi:10.1038/nature06825.

Flückiger, J., T. Blunier, B. Stauffer, J. Chappellaz, R. Spahni, K. Kawamura, J. Schwander, T. F. Stocker, and D. Dahl-Jensen (2004), N_2O and CH_4 variations during the last glacial epoch: Insight into global processes, *Global Biogeochem. Cycles*, *18*, GB1020, doi:10.1029/2003GB002122.

Ganopolski, A., and S. Rahmstorf (2001), Rapid changes of glacial climate simulated in a coupled climate model, *Nature*, *409*, 153–158, doi:10.1038/35051500.

Guenther, A., et al. (1995), A global model of natural volatile organic compound emissions, *J. Geophys. Res.*, *100*(D5), 8873–8892, doi:10.1029/94JD02950.

Harder, S. L., D. T. Shindell, G. A. Schmidt, and E. J. Brook (2007), A global climate model study of CH_4 emissions during the Holocene and glacial-interglacial transitions constrained by ice core data, *Global Biogeochem. Cycles*, *21*, GB1011, doi:10.1029/2005GB002680.

Hopcroft, P. O., et al. (2011), Simulating idealized Dansgaard-Oeschger events and their potential impacts on the global methane cycle, *Quat. Sci. Rev.*, *30*, 3258–3268, doi:10.1016/j.quascirev.2011.08.012.

Huber, C., et al. (2006), Isotope calibrated Greenland temperature record over Marine Isotope Stage 3 and its relation to CH_4, *Earth Planet. Sci. Lett.*, *243*, 504–519, doi:10.1016/j.epsl.2006.01.002.

Jones, C., et al. (2005), Systematic optimisation and climate simulation of FAMOUS, a fast version of HadCM3, *Clim. Dyn.*, *25*, 189–204, doi:10.1007/s00382-005-0027-2.

Kaplan, J. O., G. Folberth, and D. A. Hauglustaine (2006), Role of methane and biogenic volatile organic compound sources in late glacial and Holocene fluctuations of atmospheric methane concentrations, *Global Biogeochem. Cycles*, *20*, GB2016, doi:10.1029/2005GB002590.

Köhler, P., et al. (2010), What caused Earth's temperature variations during the last 800,000 years? Data-based evidence on radiative forcing and constraints on climate sensitivity, *Quat. Sci. Rev.*, *29*, 129–145, doi:10.1016/j.quascirev.2009.09.026.

Lawrence, M. G., et al. (2001), What does the global mean OH concentration tell us?, *Atmos. Chem. Phys.*, *1*, 37–49, doi:10.5194/acp-1-37-2001.

Lelieveld, J., et al. (2008), Atmospheric oxidation capacity sustained by a tropical forest, *Nature*, *452*, 737–740, doi:10.1038/nature06870.

Levine, J. G., E. W. Wolff, A. E. Jones, L. C. Sime, P. J. Valdes, A. T. Archibald, G. D. Carver, N. J. Warwick, and J. A. Pyle (2011a), Reconciling the changes in atmospheric methane sources and sinks between the Last Glacial Maximum and the pre-industrial era, *Geophys. Res. Lett.*, *38*, L23804, doi:10.1029/2011GL049545.

Levine, J. G., et al. (2011b), In search of an ice-core signal to differentiate between source-driven and sink-driven changes in atmospheric methane, *J. Geophys. Res.*, *116*, D05305, doi:10.1029/2010JD014878.

Lieth, H. (1975), Modeling the primary productivity of the world, in *Primary Productivity of the Biosphere*, edited by H. Lieth and R. Whittaker, pp. 237–264, Springer, New York, doi:10.1007/978-3-642-80913-2_12.

Loulergue, L., et al. (2008), Orbital and millennial-scale features of atmospheric CH_4 over the past 800,000 years, *Nature*, *453*, 383–386, doi:10.1038/nature06950.

Marti, J., and K. Mauersberger (1993), Laboratory simulations of PSC particle formation, *Geophys. Res. Lett.*, *20*, 359–362, doi:10.1029/93GL00083.

McManus, J. F., et al. (2004), Collapse and rapid resumption of Atlantic meridional circulation linked to deglacial climate changes, *Nature*, *428*(6985), 834–837, doi:10.1038/nature02494.

Peeters, J., et al. (2009), HO_x radical regeneration in the oxidation of isoprene, *Phys. Chem. Chem. Phys.*, *11*, 5935–5939, doi:10.1039/b908511d.

Pöschl, U., et al. (2000), Development and intercomparison of condensed isoprene oxidation mechanisms for global atmospheric modeling, *J. Atmos. Chem.*, *37*, 29–52, doi:10.1023/A:1006391009798.

Possell, M., et al. (2005), The effects of glacial atmospheric CO_2 concentrations and climate on isoprene emissions by vascular plants, *Global Change Biol.*, *11*, 60–69, doi:10.1111/j.1365-2486.2004.00889.x.

Power, M. J., et al. (2008), Changes in fire regimes since the Last Glacial Maximum: An assessment based on a global synthesis and analysis of charcoal data, *Clim. Dyn.*, *30*, 887–907, doi:10.1007/s00382-007-0334-x.

Singarayer, J. S., et al. (2011), Late Holocene methane rise caused by orbitally controlled increase in tropical sources, *Nature*, *470*, 82–85, doi:10.1038/nature09739.

Singarayer, J. S., and P. J. Valdes (2010), High-latitude climate sensitivity to ice-sheet forcing over the last 120 kyr, *Quat. Sci. Rev.*, *29*, 43–55, doi:10.1016/j.quascirev.2009.10.011.

Smith, R., et al. (2008), A description of the FAMOUS (version XDBUA) climate model and control run, *Geosci. Model Dev.*, *1*, 53–68, doi:10.5194/gmd-1-53-2008.

Spahni, R., et al. (2005), Atmospheric methane and nitrous oxide of the late Pleistocene from Antarctic ice cores, *Science*, *310*, 1317–1321, doi:10.1126/science.1120132.

Stockwell, D. Z., et al. (1999), Modelling NO_x from lightning and its impact on global chemical fields, *Atmos. Environ.*, *33*, 4477–4493, doi:10.1016/S1352-2310(99)00190-9.

Stouffer, R. J., et al. (2006), Investigating the causes of the response of the thermohaline circulation to past and future climate changes, *J. Clim.*, *19*(8), 1365–1387, doi:10.1175/JCLI3689.1.

Valdes, P. J., D. J. Beerling, and C. E. Johnson (2005), The ice age methane budget, *Geophys. Res. Lett.*, *32*, L02704, doi:10.1029/2004GL021004.

Weber, S. L., A. J. Drury, W. H. J. Toonen, and M. van Weele (2010), Wetland methane emissions during the Last Glacial Maximum estimated from PMIP2 simulations: Climate, vegetation, and geographic controls, *J. Geophys. Res.*, *115*, D06111, doi:10.1029/2009JD012110.

Woodward, F. I., T. M. Smith, and W. R. Emanuel (1995), A global land primary productivity and phytogeography model, *Global Biogeochem. Cycles*, *9*(4), 471–490, doi:10.1029/95GB02432.